where $\mathfrak{F}_2$ and $\mathfrak{F}_1$ are Fermi-Dirac integrals of dimensionless form.[8] Based on this model, the Fermi level is found to lie 0.021 eV above the conduction band edge. Acoustic lattice scattering and impurity scattering yield values of V_F which are not consistent with results of resistivity and Hall measurements (a high density of carriers at temperatures down to 4.2°K), and only optical lattice scattering gives approximately the correct temperature dependence of mobility at 300°K.

III. CONCLUSION

The results of resistivity, Hall, and thermoelectric measurements conclusively show that CsAu is an n-type semiconductor. The negligible change in resistivity at temperatures down to 4.2°K and the high density of carriers (10^{18}–10^{19} cm^{-3}) suggest that the broadening of cesium donor levels is so great as to overlap the main conduction band. The Seebeck coefficient shows that the Fermi level lies about 0.02 eV above the conduction band edge.

[8] J. S. Blakemore, *Semiconductor Statistics* (Pergamon Press Inc., New York, 1962).

ACKNOWLEDGMENTS

We are grateful to W. E. Spicer for many helpful discussions pertaining to both theory and experiment. Thanks are due A. L. Greilich and T. G. Brown for tube construction, and C. M. Howard, D. D. Wood, and A. Harral for help with the experiments.

PHYSICAL REVIEW VOLUME 131, NUMBER 2 15 JULY 1963

Stark Effect and Hyperfine Structure of Hydrogen Fluoride*

RAINER WEISS†

Research Laboratory of Electronics, Massachusetts Institute of Technology, Cambridge, Massachusetts
and
Tufts University, Medford, Massachusetts

(Received 8 March 1963)

The nuclear hyperfine structure constants and the electric dipole moment of hydrogen fluoride, H^1F^{19}, in the ground-vibration and first excited rotation state have been measured in a molecular beam electric resonance experiment. The hfs constants are: $c_F=307.6\pm1.5$ kc/sec, $c_p=-70.6\pm1.3$ kc/sec, $\frac{2}{3}g_pg_F\mu_{nm}^2/h\langle r^3\rangle=57.6\pm0.44$ kc/sec. The apparatus was calibrated by observing Stark transitions in the ground-vibration and first excited rotation state of carbonyl sulfide, $O^{16}C^{12}S^{32}$, which gave $\mu_{HF}/\mu_{OCS}=2.554\pm0.0037$, or $\mu_{HF}=1.8195\pm0.0026$ D, by using $\mu_{OCS}=0.7124\pm0.0002$ D. An absolute measurement of the OCS electric dipole moment gave $\mu_{OCS}=0.7120\pm0.003$ D. A digitally computed solution of the Stark effect with magnetic hyperfine structure was necessary to interpret the data. The theory and experiment are in good agreement over the range of electric-field strengths used in the experiment. The hfs constants are in excellent agreement with the averaged absolute values of these constants as measured in a molecular beam magnetic resonance experiment. The agreement has significance because of discrepancies between the results from the two resonance methods, for some other molecules, in previous experiments.

INTRODUCTION

IT seemed interesting to do an electric resonance experiment on HF for the following two reasons: (1) To date, no unambiguous measurement of the electric dipole has been made even though it has been subject to extensive calculations[1,2]; (2) Baker *et al.*[3] have determined the average absolute values of the spin-spin and spin-rotation interaction constants from an almost completely resolved spectrum in a molecular beam magnetic resonance experiment. A comparison of their results with those from an electric resonance experiment might indicate if there is really something fundamental in the discrepancies between results from the two resonance methods for some other molecules in previous experiments.[4]

THEORY

An adequate Hamiltonian for HF in an external electric field is

$$H=H_0+H_N+H_E,$$

where

$$H_N/h=c_F\mathbf{I}_F\cdot\mathbf{J}+c_p\mathbf{I}_p\cdot\mathbf{J}+\frac{g_Fg_p\mu_{nm}^2}{\langle r^3\rangle(2J+3)(2J-1)}\times[3(\mathbf{I}_F\cdot\mathbf{J})(\mathbf{I}_p\cdot\mathbf{J})+3(\mathbf{I}_p\cdot\mathbf{J})(\mathbf{I}_F\cdot\mathbf{J})-2\mathbf{I}_F\cdot\mathbf{I}_pJ(J+1)],$$

and

$$H_E=-\mathfrak{y}(J,v)\cdot\mathcal{E}-\tfrac{1}{2}\alpha_{z'z'}\mathcal{E}_z^2-\tfrac{1}{2}(\alpha_{z'z'}-\alpha_{x'x'})\mathcal{E}_z^2\cos^2\theta.$$

* This work was supported in part by the U. S. Army, the Air Force Office of Scientific Research, and the Office of Naval Research.

† Present address: Physics Department, Princeton University, Princeton, New Jersey.

[1] A. M. Karo and L. C. Allen, J. Chem. Phys. **31**, 968 (1959).

[2] R. K. Nesbet, J. Chem. Phys. **36**, 1518 (1962).

[3] M. R. Baker, M. Nelson, J. A. Leavitt, and N. F. Ramsey, Phys. Rev. **121**, 807 (1961).

[4] J. C. Swartz and J. W. Trischka, Phys. Rev. **88**, 1085 (1952).

H_0 involves the kinetic energies and Coulomb interactions of the nuclei and electrons which comprise the molecule. It yields the electronic, vibrational, and rotational energies. H_N and H_E are treated as perturbations. H_N describes the nuclear hyperfine structure; the first and second terms are the interactions between nuclear magnetic moments and the magnetic field induced by the molecular rotation-spin rotation interactions. The third term is the interaction of one nuclear magnetic moment in the magnetic field of the other-spin-spin interaction. H_E describes the electric dipole interaction between the external electric field and the molecular charge distribution. The first term is due to a permanent electric dipole moment, μ, that lies along the internuclear axis. μ is a function of the internuclear separation which changes slightly with rotation and vibration state. The second and third terms are due to a dipole induced in the molecular charge distribution by the external field, the so-called distortion polarization. $\alpha_{j'j'}$ is the molecular polarizability tensor which is diagonal in a molecule fixed coordinate system where the z' axis lies along the internuclear line.

H_E commutes with J_z and does not operate on the nuclear spins; it is, therefore, diagonal in a m_I, m_J representation.[5] The $\boldsymbol{\mu}\cdot\boldsymbol{\mathcal{E}}$ term mixes neighboring J states and gives second-order and higher even-order perturbation energies. The distortion polarization terms offer first order energies and are not carried to higher orders since the first-order terms are at least 1000 times smaller than those from the permanent dipole. To second order in $\boldsymbol{\mu}\cdot\boldsymbol{\mathcal{E}}$ the perturbation energies are

$$W_{E_{J\neq 0}}(J,m_J)=\frac{[\mu(J,v)\mathcal{E}]^2}{hcB_v}\left\{\left[\frac{J^2-m_J^2}{2J(2J+1)(2J-1)}-\frac{(J+1)^2-m_J^2}{2(J+1)(2J+3)(2J+1)}\right]+\frac{D_v}{B_v}\left[\frac{J(J^2-m_J^2)}{(2J+1)(2J-1)}-\frac{(J+1)(J+1)^2-m_J^2}{(2J+3)(2J+1)}\right]\right\}$$
$$-\tfrac{1}{2}(\alpha_{z'z'}-\alpha_{x'x'})\mathcal{E}^2\left\{\frac{J^2-m_J^2}{(2J+1)(2J-1)}+\frac{(J+1)^2-m_J^2}{(2J+3)(2J+1)}\right\}-\tfrac{1}{2}\alpha_{x'x'}\mathcal{E}^2,$$

$$W_E(0,0)=-\frac{1}{6}\frac{[\mu(J,v)\mathcal{E}]^2}{hcB_v}\left[1+\frac{2D_v}{B_v}\right]-\tfrac{1}{6}(\alpha_{z'z'}-\alpha_{x'x'})\mathcal{E}^2-\tfrac{1}{2}\alpha_{x'x'}\mathcal{E}^2.$$

B_v and D_v are, respectively, the rotation and centrifugal distortion constants in the vth vibration state.

H_N commutes with the z component of the total angular momentum $M_z=M_F+M_p+M_J$. The matrix of H_N in an m_I, m_J representation can, therefore, be arranged into noninteracting submatrices each associated with one value of m_z. The matrix elements themselves are easily calculable once H_N is rewritten in terms of the angular momentum ladder operators. The submatrices of H_E+H_N for the $J=1$ state are given below.

$m_z=|2|$:

m_F	m_p	m_J	$\frac{1}{2}$ $\frac{1}{2}$ 1
$\frac{1}{2}$	$\frac{1}{2}$	1	$\frac{1}{2}(c_F+c_p+\beta)+W_E(1,\|1\|)$ (H)

$m_z=|1|$:

			$\frac{1}{2}$ $\frac{1}{2}$ 0	$\frac{1}{2}$ $-\frac{1}{2}$ 1	$-\frac{1}{2}$ $\frac{1}{2}$ 1
$\frac{1}{2}$	$\frac{1}{2}$	0	$-\beta+W_E(1,0)$ (A)	$\frac{1}{2}\sqrt{2}c_p+\frac{3}{4}\sqrt{2}\beta$	$\frac{1}{2}\sqrt{2}c_F+\frac{3}{4}\sqrt{2}\beta$
$\frac{1}{2}$	$-\frac{1}{2}$	1	$\frac{1}{2}\sqrt{2}c_p+\frac{3}{4}\sqrt{2}\beta$	$\frac{1}{2}(c_F-c_p-\beta)+W_E(1,\|1\|)$ (B)	$-\beta/2$
$-\frac{1}{2}$	$\frac{1}{2}$	1	$\frac{1}{2}\sqrt{2}c_F+\frac{3}{4}\sqrt{2}\beta$	$-\beta/2$	$\frac{1}{2}(-c_F+c_p-\beta)+W_E(1,\|1\|)$ (C)

[5] Nuclear polarizabilities of either H or F are at least 10^{14} times smaller than the molecular polarizability of HF and are, therefore, neglected.

$m_z=0$:

	$\psi_+(0)$	$\psi_-(0)$	$\psi_+(1)$	$\psi_-(1)$
$\psi_+(0)$	$2\beta+W_E(1,0)$ (D)	0	$\frac{1}{2}\sqrt{2}(c_F+c_p-3\beta)$	0
$\psi_-(0)$	0	$W_E(1,0)$ (E)	0	$\frac{1}{2}\sqrt{2}(c_p-c_F)$
$\psi_+(1)$	$\frac{1}{2}\sqrt{2}(c_F+c_p-3\beta)$	0	$\frac{1}{2}(-c_F-c_p+7\beta)+W_E(1,\lvert 1\rvert)$ (F)	0
$\psi_-(1)$	0	$\frac{1}{2}\sqrt{2}(c_p-c_F)$	0	$\frac{1}{2}(-c_F-c_p-5\beta)+W_E(1,\lvert 1\rvert)$ (G)

$$\beta=g_F g_p \mu^2 \text{ nm}/5\langle r^3\rangle.$$

Submatrices associated with the same absolute value of m_z are identical because the quadratic electric field dependence allows no distinction between states that are merely reflections of each other in the external field. For the same reasons the $m_z=0$ submatrix is written in terms of the superposition of degenerate states

$$\psi_\pm(0)=\frac{1}{\sqrt{2}}[(\tfrac{1}{2}-\tfrac{1}{2}\quad 0)\pm(-\tfrac{1}{2}+\tfrac{1}{2}\quad 0)],$$

$$\psi_\pm(1)=\frac{1}{\sqrt{2}}[(\tfrac{1}{2}+\tfrac{1}{2}-1)\pm(-\tfrac{1}{2}-\tfrac{1}{2}+1)].$$

In this representation the diagonal terms of the $m_z=0$ matrix become directly the high-field energies.

The energies and wave functions for other field strengths were machine computed using standard programs for 4×4 and 3×3 matrices. Figure 1 shows the energy level diagram for the $J=1$ state.

Transitions

$J=0$ transitions were induced in a region where an rf electric field was applied perpendicular to a homogeneous dc field. In this configuration of fields the selection rule for electric dipole transitions is $\Delta m_z=\pm1$. A further condition, necessary for observability in the apparatus, is that the states between which the transitions occur must correspond to states with different m_j in the high-field limit. In all, seven transitions are observable, these are indicated in Fig. 1. The frequencies of the lines relative to the idealized single Stark line in the absence of hfs are plotted in Fig. 2.

Magnetic-Field Dependence of the Lines

Neglecting diamagnetic corrections, the Hamiltonian for HF due to an external magnetic field is

$$H_{\text{mag}}=-\mu_{\text{nm}}[g_J J_z+g_F I_{F_z}+g_p I_{p_z}]H_z$$
$$-\tfrac{1}{2}\mu_{\text{nm}}[(g_J J_++g_F I_{F_+}+g_p I_{p_+})H_-$$
$$+(g_J J_-+g_F I_{F_-}+g_p I_{p_-})H_+],$$

where $A_\pm=A_x\pm iA_y$.

For the case when the magnetic energy is much smaller than W_E, H_{mag} may be treated as a perturbation so that the z direction is still specified by the electric field. H_{mag} operates on the Stark and hfs perturbed wave functions.

The first term of H_{mag} yields diagonal terms that remove the degeneracy of the $|m_z|$ states in first order but do not shift the center of gravity of the states. The first-order magnetic field dependence can be used to identify some of the electric transitions; for example, at high-electric field the transitions $A-F$ and $A-G$ have the largest magnetic splittings of any of the lines. In these two transitions, the nuclear spins start parallel and turn together in the external magnetic and electric field.

The second term of H_{mag}, due to a magnetic field perpendicular to the electric field, couples states with $\Delta m_z=\pm1$ but for which only one m value changes. It gives quadratic magnetic terms that can shift the lines. As long as the coupled states are not close together, the second-order field dependence can be calculated by

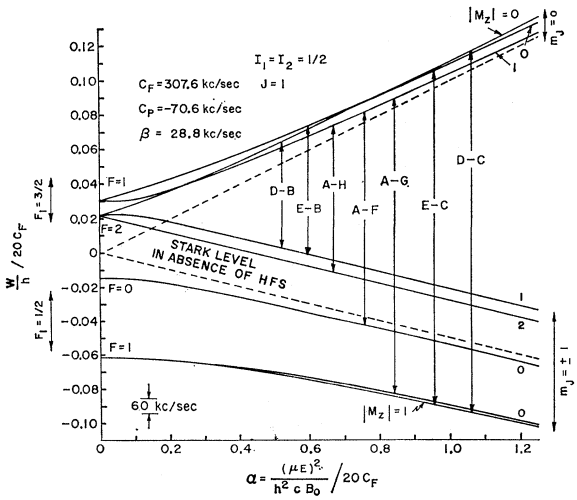

FIG. 1. Energy-level diagram of HF in the $J=1$ state in an external electric field. The letters designating the states correspond to those in the matrices given in the text.

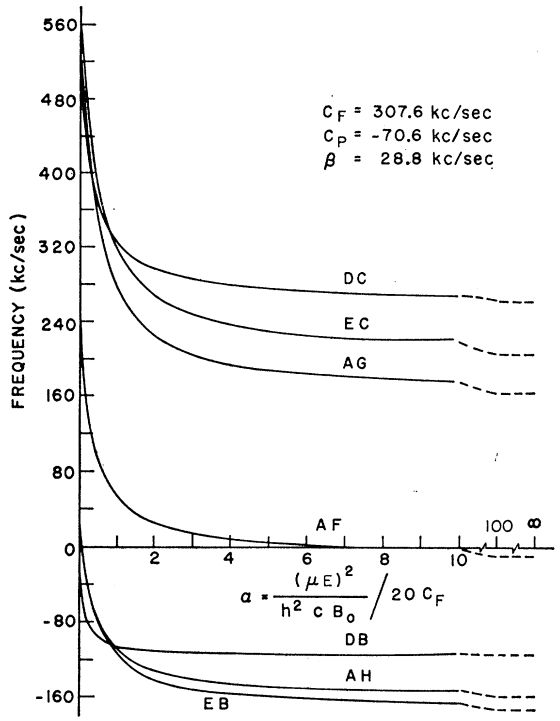

FIG. 2. Frequencies of the HF lines relative to the idealized single Stark line in the absence of hyperfine structure.

second-order perturbation theory. However, when states cross or are close together as at intermediate electric fields, the second-order field dependences are calculated by diagonalizing the submatrix of the neighboring states that are coupled by the magnetic field. Using the computer calculated wave functions and published values of g_F, g_P, g_J,[6,7] the largest second-order field dependences at $\alpha=0.5$ are

$$W_{\text{mag}}(A)=-425 \text{ cps/G}^2, \quad W_{\text{mag}}(D)=840 \text{ cps/G}^2$$
$$W_{\text{mag}}(C)=-320 \text{ cps/G}^2, \quad W_{\text{mag}}(G)=640 \text{ cps/G}^2.$$

The second-order field dependence of the other states are less than 160 cps/G².

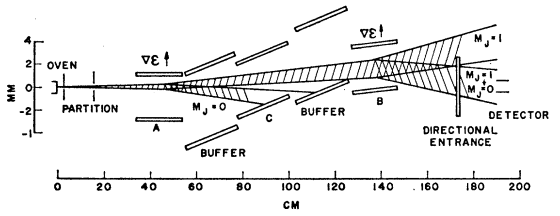

FIG. 3. Schematic view of the apparatus.

APPARATUS

A schematic view of the apparatus and the trajectories for the $J=1$ state are shown in Fig. 3. The arrangement is a flop-in experiment employing off-set geometry.[8] This method eliminates the collimator which has often been a source of Majorana transitions. The deflecting field strengths and position of an obstacle (the edge of the buffer plate nearest the B field) are so adjusted that molecules with $J>2$ are insufficiently deflected to hit the detector; however, 10% of the molecules that make the transition $J=2, m_J=|2|\rightarrow J=2, m_J=|1|$ could also pass through the apparatus.

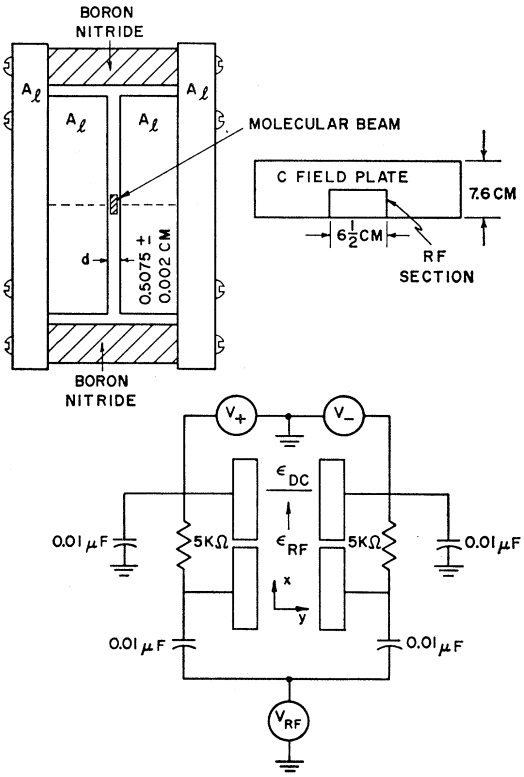

FIG. 4. The C field.

The beam emerged from the source at 225°K. At this temperature 36% of the HF molecules are in the $J=1$, $v=0$ state. The beam then passed through two pole electric deflecting fields, the electric analog of the familiar two-wire magnetic field. The C region was similar to a design of Trischka's[9] except that the rf was applied to insulated sections on both sides of the parallel plates that form the uniform field. This scheme, which is shown in Fig. 4, gives a uniform and easily calculable rf field perpendicular to the dc field. Buffer

[6] N. F. Ramsey, *Molecular Beams* (Oxford University Press, New York, 1956).

[7] C. H. Anderson, M. R. Baker, J. A. Leavitt, H. M. Nelson, J. N. Pinkerton, N. F. Ramsey, Fifth Brookhaven Conference on Molecular Beams, 1960 (unpublished).

[8] J. R. Zacharias, J. G. Yates, and R. D. Haun, Quarterly Progress Report, R. L. E., Massachusetts Institute of Technology, October 15, 1954.

[9] J. W. Trischka, Phys. Rev. 74, 718 (1948).

fields were placed between the C region and the deflecting fields in order to reduce Majorana transitions. An electron bombardment ionizer and mass spectrometer comprised the detector which has been described elsewhere.[10] The detection efficiency for HF was approximately 1/100.

EXPERIMENTAL PROCEDURE

At first, in order to narrow the line search, a crude estimate of the dipole moment was obtained by plotting the attenuation of the straight through beam as a function of A field voltage. This gave $\mu_{HF}=1.9\pm0.2$ D. Once the lines were found, they were carried to as high a field as possible before inhomogeneities in the C field broadened them beyond resolution, $\alpha\cong4$. At this field the simple analytic expressions for the high-field energies are still approximately valid. Next a magnetic field was applied parallel to the electric field in order to identify the transitions $A-F$ and $A-G$ by their large magnetic splittings. With this handle to the spectrum, the signs and approximate values of c_F, c_p, and β were calculated from the frequency intervals. At the same time K in the expression $f_{Stark}=KV^2$, where V is the

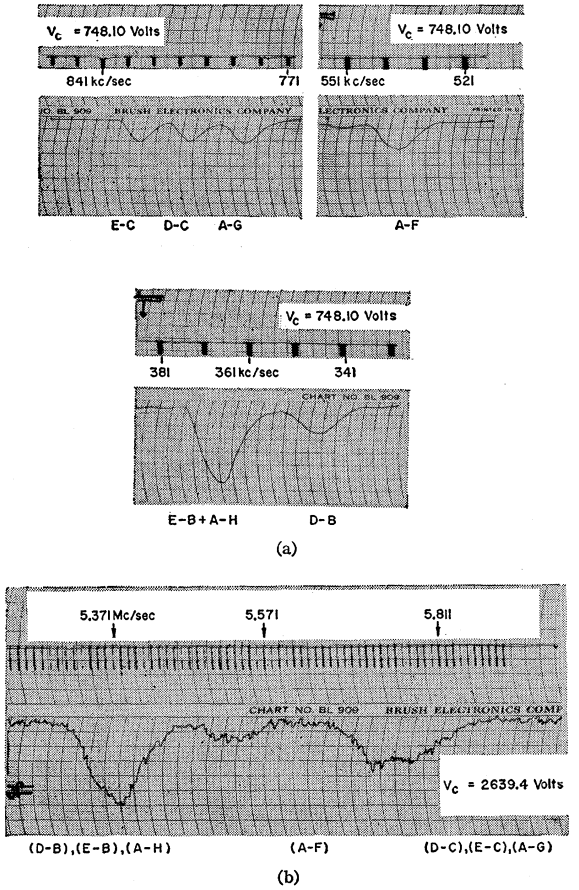

FIG. 5. (a) HF spectrum at C-field voltage of 748.10 V, which corresponds to $\alpha=0.4803$. Lock-in detector time constant, 5 sec. Down indicates increasing beam intensity. Frequency markers are 10 kc/sec apart. (b) HF spectrum at C-field voltage of 2639.4 V, which corresponds to $\alpha=5.978$. Lock-in detector time constant, 1 sec.

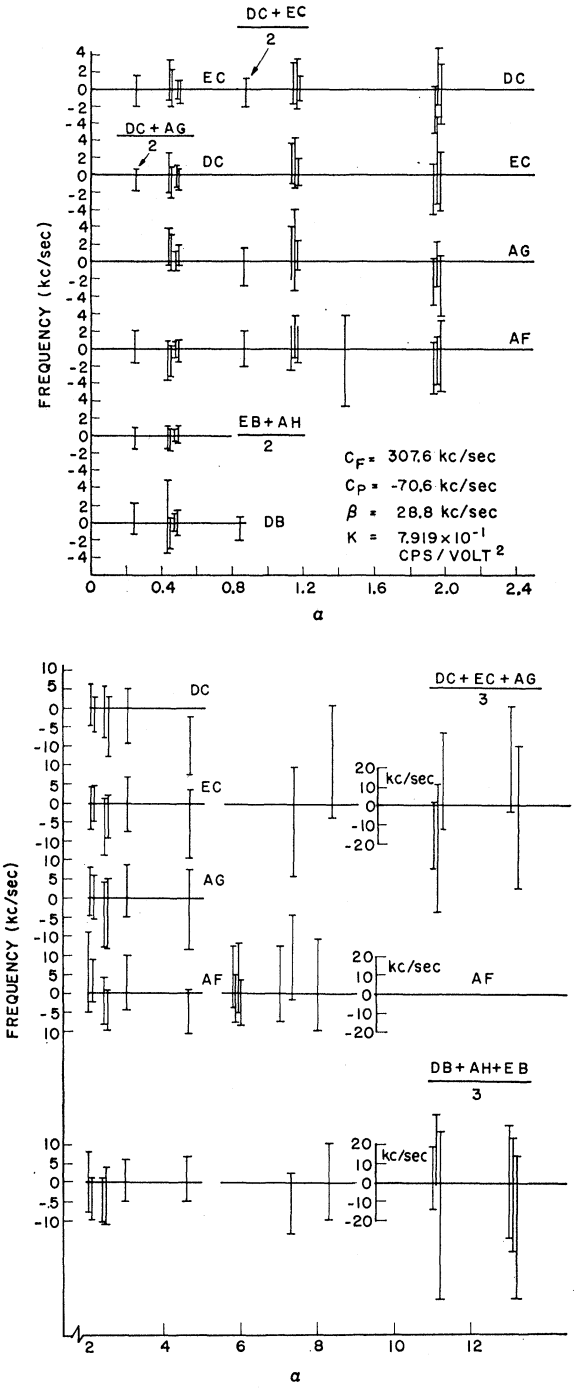

FIG. 6. All HF data plotted relative to the lines calculated by using the adopted values of the hfs constants and K_{HF}. Each point consists of two frequency scans in opposing directions.

[10] R. Weiss, Rev. Sci. Instr. 32, 397 (1961).

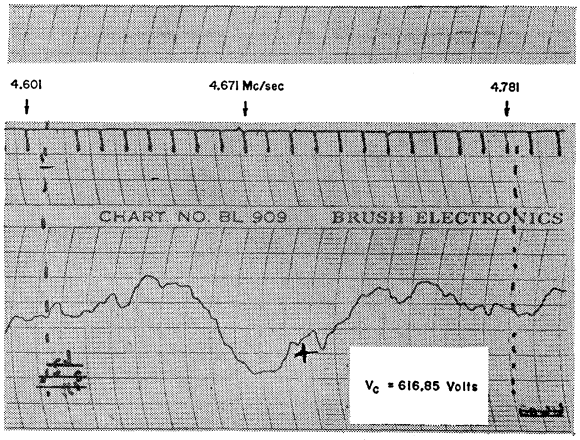

FIG. 7. Single OCS resonance at C-field voltage of 616.85 V. Lock-in detector time constant, 20 sec. Frequency markers are 10 kc/sec apart.

C-field voltage, was evaluated from the frequency of the lines with hfs terms subtracted.

These preliminary values of the hfs interaction constants were put into the computer program to calculate the energy eigenvalues for all field strengths—the energy-level diagram. This predicted line crossings at $\alpha=0.25$ and 0.85. These were observed, thereby lending confidence to the choice of the constants and, in fact, to the entire procedure.

The precise determination of the hfs interaction constants was made near $\alpha=0.5$. At this field strength all the lines are resolved except $A-H$ and $E-B$ which are superposed. In addition, the line broadening due to inhomogeneity in the C field is negligible so that the lines exhibit the anticipated 8 kc apparatus linewidth. There is, however, one difficulty with this field strength. It is an intermediate field at which no simple analytic expressions exist for the frequencies of the lines. In order to relate the data to the hfs constants, the coefficients in a Taylor expansion for the frequency intervals about $\alpha\cong 0.5$ and the approximate values of the hfs constants and K determined from the high-field data were machine computed. The expansion is

$$f_{ij}=f_{ij}|_0+\left[\frac{\partial f_{ij}}{\partial c_F}\bigg|_0-\frac{\partial f_{ij}}{\partial \alpha}\frac{\alpha}{c_F}\bigg|_0\right]\Delta c_F+\frac{\partial f_{ij}}{\partial c_p}\bigg|_0\Delta c_p+\frac{\partial f_{ij}}{\partial \beta}\bigg|_0\Delta\beta+\frac{\partial f_{ij}}{\partial \alpha}\frac{\alpha}{K}\bigg|_0\Delta K,$$

where f_{ij} is the frequency interval between the lines i and j. The variables are small changes in the hfs constants and K. It was generally possible to find some interval or combination of intervals which is primarily dependent on only one of the variables.

Table I shows the values of the constants determined from the various intervals. The most reliable value of $K_{HF}=(7.919\pm0.01)\times10^{-1}$ cycle/sec V^2 was determined from the line $A-F$ with hfs terms subtracted. This line remained resolved to $\alpha\cong 8$. Figure 6 shows a comparison of all the data with the lines calculated from the adopted values of the hfs constants and K. The data range over transition frequencies of 200 kc/sec → 13 Mc/sec and C-field strengths of 1000 → 6000 V/cm.

OCS Line and Dipole Moment

In order to calibrate the C field the single Stark transitions $\Delta J=0$, $\Delta m_J=\pm1$ in the $J=1$, $v_1=v_2=v_3=0$ state of $O^{16}C^{12}S^{32}$ were observed. The OCS molecular constants and dipole moment are well-known from microwave spectroscopy.[11–13] The experimental parameters were kept identical for the OCS runs except that the deflecting voltages were reduced in the ratio of $(\mu^2/B_0)_{HF}/(\mu^2/B_0)_{OCS}$. The signal to noise of the OCS resonance was not as good as for the HF. This is due to two reasons: first, at 220°K only 0.2% of the beam is in the $J=1$, $m_J=|1|$ state; and second, the detection process produced a multitude of ion fragments, so that only one fourth of the ionized beams appeared at the most useful mass number in the mass spectrometer. A typical OCS resonance is shown in Fig. 7. The average value of K_{OCS}, from data varying in frequency from 1.7 → 7 Mc/sec and C-field strength of 750 → 1500 V/cm, is $K_{OCS}=12.30\pm0.02$ cycle/sec V^2. The data were corrected for fourth-order Stark terms.

The experimental quantity K is related to the molecular constants by

$$K=\frac{W_E(1,0)-W_E(1,1)}{hd^2}=-\frac{3}{20}\frac{\mu^2(1,0)}{h^2cB_0d^2}\left[1+\frac{4}{3}\frac{D_0}{B_0}-\frac{4}{3}\frac{(\alpha_{z'z'}-\alpha_{x'x'})}{\mu^2(1,0)}hcB_0\right],$$

where d is the C-field plate separation. The second and third terms in the square bracket are much smaller than 1 and are treated as corrections. The above expression, when solved for μ and with the introduction of the measured K_{HF} and K_{OCS} along with the molecular constants given in Table II, yields the dipole mo-

TABLE I. Hyperfine structure constants evaluated from various frequency intervals. (Numerical values in kc/sec.)

From intervals	
$(DC)-(EC)+(AG)-(AF)=8\beta$[a]	$\beta=28.8\pm0.22$
$(EC)-(AG)$	$c_p=-70.7\pm2.2\pm\Delta\beta$
$(DC)-(AF)$	$c_p=-70.55\pm0.6\pm3.3\Delta\beta\pm0.07\Delta c_F$
$(AF)-(DB)$	$c_F=307.6\pm0.77\pm4.5\Delta\beta\pm0.04\Delta c_p$
$(DG)-(DB)$	$c_F=307.5\pm0.89\pm1.6\Delta\beta\pm0.6\Delta c_p$
$(EC)-(DB)$	$c_F=307.5\pm0.68\pm3.8\Delta\beta\pm1.1\Delta c_p$
$(AF)-[(AH)+(EB)]/2$	$c_F=307.6\pm0.69\pm0.4\Delta\beta\pm0.88\Delta c_p$

[a] This is true for all field strengths.

[11] M. W. P. Strandberg, T. Wentink, and R. L. Kyhl, Phys. Rev. **75**, 270 (1949).
[12] R. G. Shulman and C. H. Townes, Phys. Rev. **77**, 500 (1950).
[13] S. A. Marshall and J. Weber, Phys. Rev. **105**, 1502 (1957).

TABLE II. Pertinent molecular constants used in the calculation of the dipole moment.

HF	OCS
$B_0=20.5534\pm0.006$ cm^{-1} [a]	$B_0=6081.490$ Mc/sec[c]
$D_0=0.002114\pm0.000049$ cm^{-1} [a]	$D_0=0.00131$ Mc/sec[c]
$(\alpha_{z'z'}-\alpha_{x'x'})=2.4\times10^{-25}$ cm^3 [b]	$\mu(1,0)=0.7124\pm0.0002$ D[d]
	$(\alpha_{z'z'}-\alpha_{x'x'})=(2.4\pm3.0)\times10^{-24}$ cm^3 [d]

[a] See Ref. 16.
[b] This is the electronic polarizability anisotropy calculated by J. Clark, Nature **138**, 126 (1936). The atomic polarizability adds 2×10^{-26} cm^3 to $\alpha_{z'z'}$.
[c] C. H. Townes and A. L. Schawlow, *Microwave Spectroscopy* (McGraw-Hill Book Company, Inc., New York, 1955).
[d] See Ref. 13.

ment ratio

$$\frac{\mu(1,0)_{HF}}{\mu(1,0)_{OCS}}=2.554\pm0.0037,$$

or $\mu(1,0)_{HF}=1.8195\pm0.0026$ D. The measured gap width $d=0.5075\pm0.002$ cm so that an independent absolute determination of the dipole moments give $\mu(1,0)_{OCS}=0.7120\pm0.003$ D, $\mu(1,0)_{HF}=1.818\pm0.008$ D.

The new measurement of the OCS dipole moment is in good agreement with the two latest determinations.[12,13] The new HF dipole-moment measurement is not in agreement with previous measurements from the bulk-electric susceptibility of HF gas.[14,15] The latest of these gave $\mu_{HF}(0,0)=1.736\pm0.023$ D. The discrepancy is too large to explain by the change in dipole moment between the $J=1$ and $J=0$ states. Using Nesbet's[2] calculation of the dipole derivative $\partial\mu/\partial r=+1.03$ D/Bohr radius, the fractional change in dipole moment is $[\Delta\mu(J=1\rightarrow J=0)]/\mu=-2\times10^{-4}$. The new value of μ_{HF} is, however, in remarkable agreement with one calculated by Nesbet, $\mu_{HF_{theoretical}}=1.827$ D.[2]

HF Hyperfine Interaction Constants

The hfs interactions measured in this experiment are in excellent agreement with those determined from a molecular beam magnetic resonance experiment.

[14] N. B. Hannay and C. P. Smyth, J. Am. Chem. Soc. **68**, 171 (1946).
[15] D. W. Magnuson, Oak Ridge National Laboratory Report ORNL K-1180 (1954).

This experiment
$c_F=307.6\pm1.5$ kc/sec
$c_p=-70.6\pm1.3$ kc/sec
$2\beta=\frac{2}{5}g_pg_F\mu^2$ nm/$\langle r^3\rangle=57.6\pm0.44$ kc/sec
Magnetic resonance experiment[3]
$|\mathfrak{c}_F|=305\pm2$ kc/sec
$|\mathfrak{c}_p|=71\pm3$ kc/sec
$\frac{2}{5}g_pg_F\mu^2$ nm/$\langle r^3\rangle=57\pm2$ kc/sec.

The spin-spin interaction constant calculated from the published g values[6] and an evaluation of $1/\langle r^3\rangle$ for the $J=1$, $v=0$ state in a Morse potential using the published molecular constants[16] yields $\frac{2}{5}g_pg_F\mu^2$ nm/$\langle r^3\rangle=57.39$ kc/sec which is in good agreement with the measured value. This indicates that there is little magnetic polarization of the electrons due to the nuclear moments. The new value of c_F and c_p gives the rotational magnetic fields in the $J=1$ state at the position of the proton and fluorine nucleus as 16.6 and -76.7 G, respectively. This indicates that the proton sees primarily the magnetic field because of the rotation of the fluorine nucleus shielded by eight electrons. The fluorine nucleus, on the other hand, sees almost exclusively the magnetic field of the neighboring electrons that are coupled to the rotation because of polarization of the fluorine atomic electron structure by the electric field of the proton.

ACKNOWLEDGMENTS

I wish to thank Professor J. R. Zacharias for suggesting HF as well as for his continued interest and guidance. I am indebted to Professor J. G. King for valuable advice and to Professor W. Klemperer of the Department of Chemistry, Harvard University, for discussions concerning the theory. The help of F. J. O'Brien in the design and construction of the apparatus is much appreciated. I also thank the Computation Center, MIT, and, in particular, Miss Elizabeth J. Campbell, of the Joint Computing Group, MIT, for programming and running the intermediate field solutions.

[16] G. Kuipers, D. F. Smith, and A. H. Nielsen, J. Phys. Chem. **25**, 275 (1956).

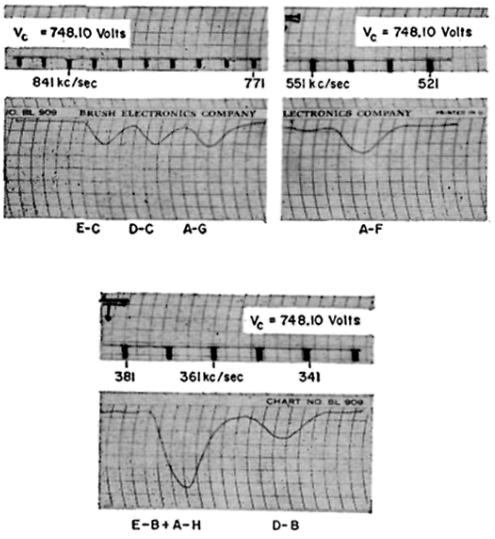

(a)

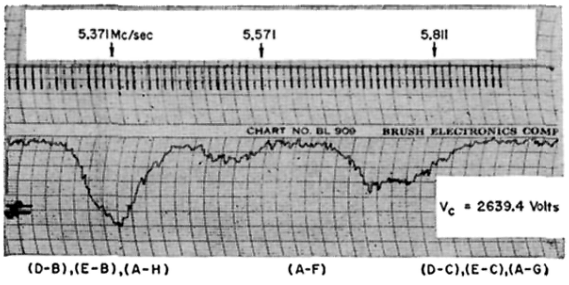

(b)

FIG. 5. (a) HF spectrum at *C*-field voltage of 748.10 V, which corresponds to $\alpha = 0.4803$. Lock-in detector time constant, 5 sec. Down indicates increasing beam intensity. Frequency markers are 10 kc/sec apart. (b) HF spectrum at *C*-field voltage of 2639.4 V, which corresponds to $\alpha = 5.978$. Lock-in detector time constant, 1 sec.

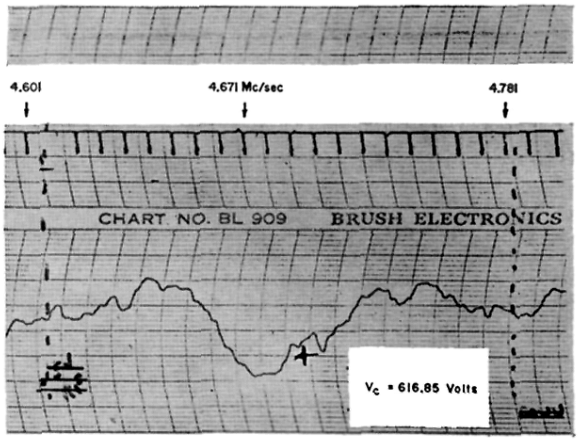

FIG. 7. Single OCS resonance at C-field voltage of 616.85 V. Lock-in detector time constant, 20 sec. Frequency markers are 10 kc/sec apart.